Nitric oxide complexes of metalloporphyrins: an overview of some mechanistic studies

Mikio Hoshino [a], Leroy Laverman [b], Peter C. Ford [b,*]

[a] *The Institute of Physical and Chemical Research, Wako, Saitama 351-0198, Japan*
[b] *Department of Chemistry, University of California Santa Barbara, Santa Barbara, CA 93106, USA*

Contents

Abstract

This review presents an overview of the mechanistic chemistry concerned with the reactions of metalloporphyrins involving the bioregulatory molecule nitric oxide. Topics discussed include the photolabilization of NO from metal nitrosyl complexes, the formation and dissociation of M–NO bonds, reductive nitrosylation of ferriheme proteins and oxidations of NO by dioxygen. Principal emphasis is given to porphyrin complexes of the first

* Corresponding author. Tel.: +1-805-8932443; fax: +1-805-8934120.
E-mail address: ford@chem.ucsb.edu (P.C. Ford)

transition row metals and especially of iron(II) and iron(III). © 1999 Elsevier Science S.A. All rights reserved.

Nomenclature

1-MeIm	1-methyl imidazole
Cat	catalase
Cyt	cytochrome-c
EDRF	endothelium derived relaxation factor
ES	electronic excited state
Φ	quantum yield
GS	ground state
Hb	ferro-hemoglobin
HOMO	highest occupied molecular orbital
LMCT	ligand to metal charge transfer
LUMO	lowest unoccupied molecular orbital
Mb	ferro-myoglobin
metMb or Mb^{III}	ferri-myoglobin
MLCT	metal to ligand charge transfer
NOS	nitric oxide synthase
OBTPP	octabromotetraphenylporphine
OEP	octaethylporphine
P	'generic' porphyrin
PPIX	protoporphyrin IX
sGC	soluble guanylyl cyclase
τ	lifetime
TMPS	tetra(sulfonatomesityl)porphine
TpivPP	picket fence porphine
TPP	meso-tetraphenylporphyrin
TPPS	tetra(4-sulfonatophenyl)porphine

1. Introduction

The reactions of synthetic metalloporphyrins with the diatomic molecules have long been of interest [1–9], interactions between iron(II) porphyrins and dioxygen receiving particular attention as models for O_2 transport and storage proteins such as hemoglobin and myoglobin [8,10–16]. However, during the past decade, considerable attention has also turned to the reactions of metalloporphyrins with nitric oxide owing to the various biological roles which now have been attributed to NO [17–29]. In a relatively short period during the late 1980s, it was reported that NO

is (1) the 'endothelium derived relaxation factor' (EDRF), a long suspected intercellular signaling agent key to the control of mammalian blood pressure, (2) a key player in cytotoxic immune response to pathogen invasion and (3) a neuro-transmission regulator in the central nervous system. Subsequent reports have identified a number of disease states involving NO imbalances [30], and such observations have stimulated extensive research into the chemistry, biology and pharmacology of NO and related compounds leading to a virtual torrent of publications in these fields.

The principal targets for NO under bioregulatory conditions are metal centers, primarily iron [31,32]. The ferroheme enzyme soluble guanylyl cyclase (sGC) is the best characterized example of such a target [33,34]. It is generally thought that formation of a nitrosyl complex with the metal center labilizes a trans axial ligand and the resulting conformational change activates the enzyme for catalytic forma-tion of the secondary messenger cyclic guanylyl monophosphate from guanylyl triphosphate. Other reports also point to NO roles in inhibition of metalloenzymes such as cytochrome P450 [35], cytochrome oxidase [36], nitrile hydratase [37–40] and catalase [41] as well as in the vasodilator properties of a salivary ferriheme protein of blood sucking insects [42]. Heme centers are also involved in the in vivo generation of NO by oxidation of arginine catalyzed by the enzymes nitric oxide synthase (NOS) [27,43,44]. For bioregulatory purposes, the NO concentrations generated are low, e.g. values of [NO] < 1 μM have been reported to be generated in endothelium cells for blood pressure control [45]. Thus, reactions with targets like sGC must be very fast to compete effectively with other physical and chemical processes leading to depletion of NO, which in vivo is suggested to have a lifetime of but a few seconds. On the other hand, the NO concentrations produced during immune response to pathogen invasion are much higher.

These biological and medical roles place a high premium on understanding the fundamental chemistry of NO under conditions relevant to its biological formation and decay. Of special interest are the reactions and interactions with metal ion centers. In this context, presented here is an overview of some developments in mechanistic chemistry involving the reactions of metalloporphyrin complexes with NO.

2. Structures and spectra of nitrosyl metalloporphyrins

A dominant theme in considering the chemistry of NO is that it is a stable free radical with an electronic structure analogous to the dioxygen cation O_2^+, i.e. the unpaired electron is located in the π^* orbital. NO reacts rapidly with other free radicals and with substitution labile redox active metals but is neither a strong one electron oxidant nor a strong one electron reductant [46]. In a complex with a metal center, the character of the NO ligand can range from that of a nitrosyl cation (NO$^+$) which binds to the metal with a M–NO angle of ~180° to that of a nitroxyl anion (NO$^-$) for which a bond angle of ~120° might be anticipated (Fig. 1). In the former case there has been considerable charge transfer to the metal and

the linearly bonded NO⁻ can be viewed as being isoelectronic to carbon monoxide. A simple description of the metal–NO interaction was offered some years ago by Feltham and Enemark [47], who proposed the {MNO}ⁿ formulation, where n is the sum of the metal d-electrons and the nitrosyl π^* electrons and used Walsh-type diagrams to predict the bond angles of this unit. When the other ligands on the metal include a strong C_{4v} perturbation, such as will always be the case with metallo porphyrins, the M–N–O angle is predicted to be linear for $n = 6$ but bent for $n > 6$. Notably, there is also a reported example of a meta-stable complex (generated photochemically in low temperature solids) which has NO coordinated at the oxygen [48] and another with an η^2-NO where the NO bond is perpendicular to metal ligand coordination axis [49].

Numerous metalloporphyrins including those of chromium, manganese, iron and cobalt, as well as various heavy metal centers react with NO to give adducts. The ability of the M(P) moiety (P = η^4-porphyrinato ligand) to form a stable NO adduct as well as the structure of that species depend strongly on the oxidation state of the metal, although assigning the metal oxidation state in the resulting adduct is subject to ambiguity. In this context, one might compare the structures of NO adducts to the metalloporphyrins Mnᴵᴵ(TPP), Feᴵᴵ(TPP) and Coᴵᴵ(TPP) (TPP = meso-tetraphenylporphyrin) which show the respective M–N–O bond angles 176.2, 142.1 and 128.5° [50–52]. The first is consistent with the nitrosyl cation formulation Mnᴵ(TPP)(NO⁺), the latter with that of the nitroxyl complex Coᴵᴵᴵ(TPP)(NO⁻), while the adduct with Feᴵᴵ(TPP) is intermediate in character. The metal–N$_{NO}$ bond lengths follow the order {Mn–NO}ⁿ (1.644 Å) < {Fe–NO}⁻ (1.717 Å) < {Co–NO}⁻ (1.833 Å) indicative of the decreasing π-bonding over this sequence. Notably, simple oxidation of the above iron adduct (i.e. to give the NO adduct of Feᴵᴵᴵ(P)) gives the {FeNO}ⁿ system which is predicted and found to be linear. Table 1 summarizes structural data for NO adducts of some Feᴵᴵ and Feᴵᴵᴵ porphyrins which have received attention as models of natural hemoproteins [52–56].

The IR spectra reflect the nature of the binding between NO and the central metal. Higher NO stretching frequencies are the rule for linear complexes such as Fe(TPP)(Cl)(NO). For example, oxidation of Fe(TPP)(NO) to Fe(TPP)(NO)⁺ in CH₂Cl₂ solution shifts ν_{NO} from 1678 to 1848 cm⁻¹ [57].

ESR spectra provide insight into the electronic structure of paramagnetic nitrosyl metalloporphyrins. For example, the manganese(III) complex, Mn(TPP)(CN) ($S = 2$) reacts with NO to give Mn(TPP)(CN)(NO) for which the ESR spectrum
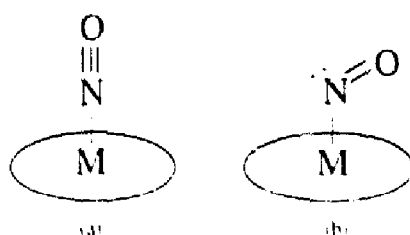

Fig. 1. Illustration of binding between a metalloporphyrin center and (a) the nitrosyl cation (NO⁺) or (b) nitroxyl (NO⁻).

Table 1

Fe NO bond distances and Fe N O angles of nitrosyl iron porphyrins determined by X-ray crystallography

Complex	Fe NO (Å)	Fe N O angle (°)	ν_{NO} (cm^{-1})	Ref.
Fe^{II}(TPP)(NO)	1.717	149.2	1670	[53]a
Fe^{II}(TPP)(NO)(4MePip)	1.740	143.7	1653	[53]b
Fe^{II}(T$_{piv}$PP)(NO)^a	1.716	143 (131)	1665	[54]
Hb(NO)^b	1.74	145		[55]
Fe^{II}(TPP)(N)(NO)^c	1.743	142.1 (138.3)	1625	[56]
[Fe^{III}(TPP)(H$_2$O)(NO)]^d	1.652	174	1848 [57]	[52]
[Fe^{III}(OEP)(NO)]^e	1.644	176.9	1862	[52]

^{a} TpivPP = picket fence porphyrin.
^{b} Hb = ferro-hemoglobin (Ref. [33]).
^{c} N = N-methylimidazole.
^{d} [Fe^{III}(TPP)(NO)]$^+$ = [Fe^{III}(TPP)(NO)][ClO$_4$].
^{e} [Fe^{III}(OEP)(NO)]$^+$ = [Fe^{III}(OEP)(NO)][ClO$_4$]; OEP = octaethyl porphyrin.

indicates a low spin state, $S = 1\ 2$ [3]. Similarly, the NO adduct of the chromium(II), Cr^{II}(TPP) ($S = 2$), exhibits an ESR spectrum consistent with a $S = 1\ 2$ spin state [3], while reaction of NO with Mn^{II}(TPP) ($S = 5/2$) [58,59] gives an adduct with $S = 0$ [3]. Thus, NO coordination gives strong field complexes with such metal centers. However, one-electron reduction of Mn^{II}(TPP)(NO) (by radiolysis in 2-methyltetrahydrofuran solution) gives [Mn^{II}(TPP)(NO)] which exhibits the ESR spectrum of a $S = 3\ 2$ state at 77 K [60].

The ESR spectra of nitrosyl Fe^{II} porphyrins (Fe^{II}(P)(NO)) clearly show the super hyperfine splitting due to the nitrogen atom of the axial NO, indicating that the unpaired electron density is concentrated at the d orbital of the central iron atom [61 65]. The spectra display three unique g values consistent with the non-axial symmetry and the bent-form of the Fe N O moiety, in accordance with the X-ray structure determination (Table 1). For nitrosyl adducts of ferrohemoproteins having a histidine residue in the axial site, ESR spectra display the N hyperfine splitting of both NO and the imidazole moiety of histidine [64].

The electronic absorption spectra of nitrosyl metalloporphyrins are dominated by the π-π^* ligand bands which constitute the spectra of other metalloporphyrins as well as the free base ligand. In the four orbital model of Gouterman there are two ligand π HOMOs of a_{1u} and a_{2u} symmetry and two π^* LUMOs of e_g symmetry [66]. Constructive and destructive mixing of these orbitals results in electronic absorption spectra with two principal types of bands. The Soret (or B) band is dominant band in the ~350 450 nm range and has extinction coefficients to $> 10^5$ M^{-1} cm^{-1}. To the red of the Soret band (~500 700 nm) are two 'weaker' bands which display extinction coefficients to $> 10^4$ M^{-1} cm^{-1}. The lower energy of these is the Q_0 band; the higher energy absorption includes one mode of vibrational excitation and is denoted Q_1. The optical absorption spectrum of the metalloporphyrins may exhibit weaker electronic transitions including charge transfer transitions (LMCT or MLCT) between the porphyrin ligand and the metal or metal centered σ –

transitions. Also of particular interest to the photochemistry of nitrosyl complexes are excited states resulting from charge transfer transitions between the metal and the NO ligand. However, from a qualitative perspective, the absorption spectra of metalloporphyrins are dominated by the Soret and Q bands, and how these are affected by the metal and axial ligands are reviewed elsewhere [66].

3. Photolabilization of nitrosyl metalloporphyrins

3.1. Quantum yields

Photochemical reactions of nitrosyl metallo porphyrins and metallo-proteins were research topics long before the biological roles of NO were recognized [67]. For example, Hoffman and Gibson in 1978 reported conventional flash lamp photolysis studies (pulse duration ~ 400 μs), of the O_2, NO, and CO complexes of myoglobin (Mb, having a ferroheme center) and the metal substituted myoglobins, $Mn^{II}Mb$ and $Co^{II}Mb$ [68]. A quantum yield (Φ_{dis}) of unity was reported for photodissociation of CO from its Mb complex and of NO from its $Mn^{II}Mb$ and met–myoglobin ($Fe^{III}Mb$) complexes, but the yields seen for NO and O_2 photodissociation from their respective complexes with Mb were quite small ($< 10^{-3}$ and $< 10^{-2}$) as were those for the $Co^{II}Mb(NO)$ and $Co^{II}Mb(O_2)$ complexes (both $< 10^{-1}$). In this context, it was suggested that the quantum yield of XY labilization could be correlated with r, the total number of electrons in the metal d-orbitals and ligand π^* orbitals (r is equivalent to the n value described above for $\{MNO\}^n$). Large Φ_{dis} were seen when $r = 6$ and small values when $r > 6$.

Subsequently, Rose and Hoffman [69] measured quantum yields for NO photodissociation from iron protoporphyrin IX 1-methylimidazole nitrosyl, $FePP(1-MeIm)(NO)$, in aqueous solutions using ns laser techniques (Eq. (1), P = PP) and found excitation wavelength independent Φ_{dis} values of 0.1, much larger than for the protein but still significantly less than unity. They interpreted the much larger value in this case relative to that for the Mb(NO) complex in terms of a model in which NO photolabilization first gives a (heme, NO) 'encounter pair' surrounded by a solvent cage or embedded in the protein pocket. Dissociation of the (heme, NO) pair is presumed to be much more facile for the model heme complex than from the protein heme pocket, thus the latter undergoes recombination much more readily than it does diffusion apart to give net ligand labilization. The influence of protein structure on the efficiency and dynamics of the ligand (NO) escape to the bulk solution relative to recapture by the metal has been the stimulus of several ultra fast kinetics studies of various myoglobin complexes modified by site directed mutagenesis (see below) ([63]b).

$$M(P)(NO) \xrightarrow{h\nu / I_a} M(P) + NO \qquad\qquad (1)$$
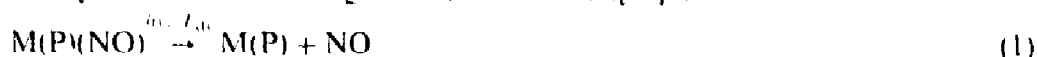
The much higher photolability of nitrosyl metalloporphyrins in the absence of the protein was further demonstrated by ns laser flash photolysis (355 nm) studies [70,71] of the Mn^{II}, Fe^{II} and Co^{II} tetraphenylporphyrin complexes M(TPP)(NO) in

300 K benzene solution. In all three cases, Φ_{di} values for NO photolabilization (Eq. (1), P = TPP) proved to be quite large (0.78, 0.5 and 1.0, respectively), the latter two being dramatically higher than in the myoglobin derivatives. Similarly, the photolability of NO from its complex with $Fe^{II}(TPPS)$ (TPPS = tetra(4-sulfonatophenyl)porphine) has been shown to have a Φ_{di} of 0.16 in aqueous solution [68]. Thus, the electronic argument regarding r may not be sufficient to explain the observed photolabilities of the different nitrosyl complexes. Certainly, mechanical effects resulting from the presence of the protein play a major role, at least for the Mb and $Co^{II}Mb$ complexes, and, as will be noted below, a similar argument has been offered to interpret the low quantum yield for photodissociation from oxyhemoglobin [72]. On the other hand it is notable that such mechanical effects do not dominate the behavior of the analogous $Mn^{II}Mb$ and $Fe^{III}Mb$ species.

Before further discussion of published studies of the quantum yields and dynamics of NO photolabilization from M(P)(NO) complexes, it may be valuable to construct a model such as illustrated by Fig. 2 as the initial basis for such discussion. In this model one may envision several stages in NO photodissociation. The first of course is the formation of the initial electronic excited state (ES_i) upon absorption of light by the ground state (GS) of M(P)(NO). This is followed by internal conversion intersystem crossing (k_{ic}) to give the reactive excited state (ES_r) in competition with deactivation directly to GS (k_{nr1}) with an efficiency strictly dependent on the photophysical processes $(\Phi_{ic} = k_{ic}/(k_{ic} + k_{nr1}))$. From ES_r, bond dissociation to give the caged geminate pair $\{M(P), NO\}$ (k_1) may occur in competition with deactivation to GS (k_{nr2}) with the net efficiency $\Phi_{gp} = \Phi_{ic}(k_1/(k_1 + k_{nr2}))$. In the same context, the geminate pair may reform the M–NO bond (k_{gp}) to give GS or evolve further to a solvent separated encounter pair $\{M(P)::NO\}$ (k_2) with an overall efficiency $\Phi_{es} = \Phi_{gp}(k_2/(k_2 + k_{ic}))$. Lastly, $\{M(P)::NO\}$ may recombine via some type of activated pathway to reform M(P)(NO) or diffuse apart (k_{-d}) to M(P) plus NO (the term k_d represents the rate constant for the reverse process simple bimolecular diffusion in solution to reform the encounter pair, a likely first step in the thermal reaction pathway for reforming the nitrosyl complex, see Fig. 2).

For such a model, the quantum yield is clearly dependent upon the process being evaluated and upon the time interval of observation. For example, under continuous photolysis conditions with relatively low intensity light, the steady state concentrations of none of the potentially observable species formed along the photochemical reaction coordinate, including the fully separated M(P) plus NO, may be measurable, so the apparent Φ_{di} may approximate zero under such conditions. On the other hand, certain species may be directly observable using flash photolysis techniques with the appropriate time resolution. In particular, on the time scale of ns and µs flash experiments, especially in the absence of added NO, the second order back reaction of M(P) plus NO is relatively slow, and this allows one to determine the true Φ_{di} of M(P) formation. According to the model, this would equal $\Phi_{es}(k_{-d}/(k_{-d} + k_2))$, and in fluid solutions, one might anticipate that for simple metalloporphyrins such as the complexes of PPIX, TPP and TPPS, k_{-d} would be quite rapid relative to k_2, i.e. $\Phi_{di} = \Phi_{es}$. However, in the encumbering environment of a metalloprotein, k_{-d} (and possibly k_2) might be expected to be

$$ES_1 \quad \overset{k_{ic}}{\sim\!\!\!\!\longrightarrow} \quad ES_r \quad \overset{k_1}{\longrightarrow} \quad \{M(P).NO\} \quad \overset{k_2}{\longrightarrow} \quad \{M(P)::NO\} \quad \overset{k_{-d}}{\underset{k_d}{\rightleftharpoons}} \quad M(P_1)+NO$$
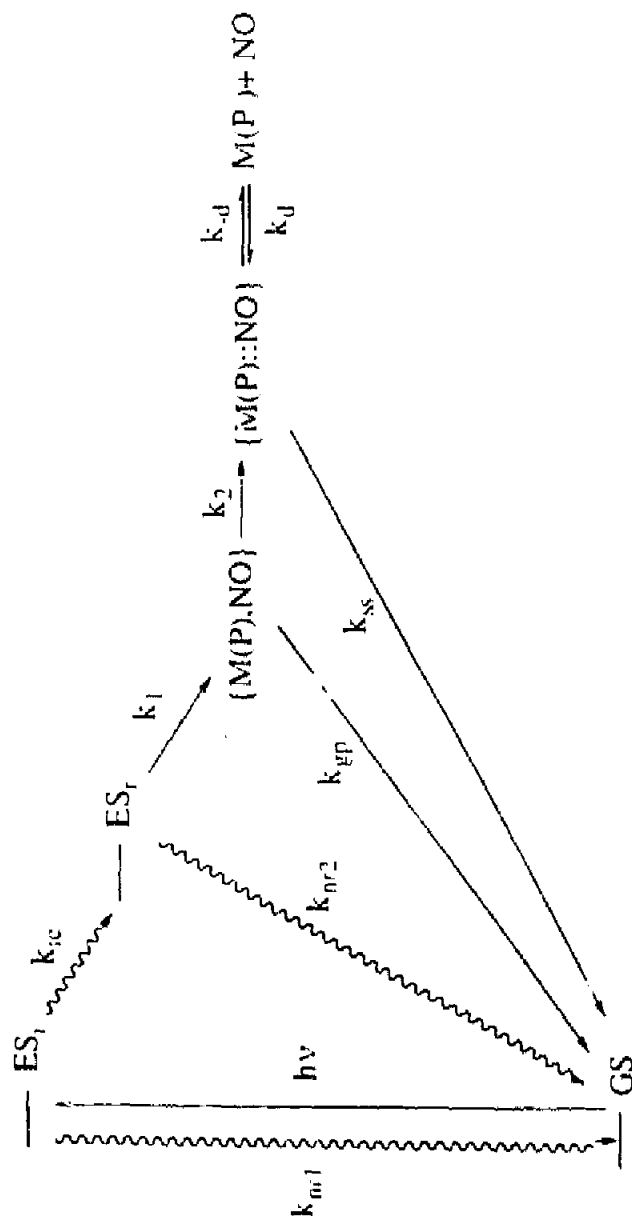
Fig. 2. Possible scheme for the photodissociation of NO from a metal porphyrin nitrosyl $M(P)(NO)$.

substantially slowed. If so, Φ_{dis} would be smaller (as observed) relative to the appropriate nitrosyl metalloporphyrins models.

A similar quantum yield study of NO photolabilization has been reported for the NO adducts of the water soluble nitrosyl iron(III) porphyrin Fe^{III}(TPPS) and of some ferrihemoproteins in aqueous solution. Each of these reacts reversibly with NO to give the respective nitrosyl adducts and the equilibrium constants are small enough to measure by conventional spectroscopic titration (see below) [73]. The 355 nm laser flash photolysis of Fe^{III}(TPPS)(NO) in pH 6.5 solution gives rise to the formation of Fe^{III}(TPPS) and NO with a Φ_{dis} of 0.37. By comparison, the quantum yields for photodissociation of NO from the nitrosyl ferrihemoproteins proved to be significantly smaller with Φ_{dis} values of 0.027 measured for Mb^{III}(NO) (Mb^{III} = metmyoglobin), 0.034 for Cyt^{III}(NO) (Cyt^{III} = ferri-cytochrome-c) and 0.05 for Cat^{III} (Cat^{III} = catalase) [73]. The smaller yields for these nitrosyl ferrihemoproteins can be attributed to the effects of the protein surrounding the heme, i.e. most of the NO once photodissociated is captured in the protein pocket without diffusing out of the hemoproteins and immediately returns to regenerate the NO adducts. It is notable that these nitrosyl ferriheme proteins are considerably more labile both photochemically and thermally toward NO dissociation than their ferroheme analogs.

Cyt^{III} has a six coordinated structure in which methionine S is tightly bound to the central iron atom [74], and thus, Cyt^{III} is expected to accompany a large change in the protein conformation before and after nitrosylation. The laser photolysis studies of Cyt^{III}(NO) have revealed that the transient spectrum detected at 50 ns after the laser pulse is ascribed to Cyt_{ri}^{III} which relaxes to Cyt^{III} with the first order rate constant 5.5×10^3 s^{-1}, suggesting that Cyt_{ri}^{III} produced immediately after the photodissociation of NO from Cyt^{III}(NO) changes the conformation with time and eventually relaxes to Cyt^{III} [73]. This system would appear to be ripe for more detailed study by ps and fs photolysis methods. Such protein conformation changes have also been reported to accompany photodissociation of O_2 from oxymyoglobin under ns laser photolysis [75].

Temperature effects on quantum yields for NO dissociation have been probed for the three model complexes Fe^{II}(TPP)(NO), Co^{II}(TPP)(NO), and Mn^{II}(TPP)(NO) in toluene solutions over the temperature range 180–300 K [71]. The Φ_{dis} values for both Fe^{II} and Co^{II} species were independent of excitation wavelength but fell as the temperature was lowered, the former decreasing from 0.50 to 0.10 over this range, the latter from 1.0 to 0.40. On the other hand, that for Mn^{II}TPP(NO) (Φ_{dis} = 0.78 for 355 nm excitation; 0.63 for 532 nm) exhibited no temperature dependence. Two possible general explanations of temperature dependent Φ_{dis} values would be: (i) the increase in solvent viscosity at low temperatures inhibits diffusion of photodissociated fragments from the solvent cage so that the efficiency of the geminate recombination increases and or (ii) an activation energy is necessary for axial ligand dissociation from the reactive excited state. If (i) were dominant, similar temperature-dependence among Fe^{II}(TPP)(NO), Co^{II}(TPP)(NO), and Mn^{II}(TPP)(NO) could be expected, and this was not the case. Therefore, (ii) was chosen [71] as the model to interpret the temperature dependencies of the quantum yields. From (ii),

the quantum yield for NO dissociation is expressed by:

$$\Phi_{dis} = \Phi_{ic}\left(\frac{k_{dis}}{k_{nr2} + k_{dis}}\right) \tag{2}$$

where (using terms consistent with Fig. 2) Φ_{ic} is the yield of the reactive excited state ES_r and k_{nr2} is the rate constant for non-radiative decay of ES_r and k_{dis} a rate constant for the dissociation of NO from ES_r to give the separated species M(P) plus NO. According to the discussion of Fig. 2,

$$k_{dis} = k_1\left(\frac{k_2}{k_2 + k_{gp}}\right)\left(\frac{k_{-d}}{k_{-d} + k_{ss}}\right) \tag{3}$$

which simplifies to $k_{dis} = k_1$, if $k_2 \gg k_{gp}$ and $k_{-d} \gg k_{ss}$. With regard to temperature dependence, k_{dis} can be formulated as

$$k_{dis} = k_{dis}^0 \exp(-\Delta E_r/RT) \tag{4}$$

where ΔE_r is the activation energy for the dissociation of the ligand at the reactive state, and k_{dis}^0 is effectively the Arrhenius frequency factor. From Eqs. (2) and (4), one obtains

$$\Phi_{dis} = \Phi_{ic}[1 + k_{nr2}/k_{dis}^0 \exp(-\Delta E_r/RT)]^{-1} \tag{5}$$

The temperature dependence of Φ_{dis} over the range 180–300 K for Fe^{II}TPP(NO) and Co^{II}TPP(NO) could be fit well to this mathematical model given the assumption that $\Phi_{ic} = 1.0$ and the respective ΔE_r values 10 and 22 kJ mol^{-1} [71]. Based on the same assumptions, the temperature dependence of Φ_{ic} for Co^{II}(OEP)(NO) (OEP = octaethylporphyrin) gave a ΔE_r (18 kJ mol^{-1}) comparable to that of its TPP analog, but ΔE_r proved to be about zero for both Mn^{II}(TPP)(NO) and Mn^{II}(OEP)(NO). The Mn^{II} complexes are linear {MNO}^{6} species while the Fe^{II} and Co^{II} complexes have the bent {MNO}^{7} and {MNO}^{8} structures, respectively, the temperature dependence results have been interpreted in terms of ES_r being a dissociative state for the $n = 6$ Mn^{II} complexes. An activation energy ΔE_r, which increases as the MNO bond angle decreases, is required to labilize NO from ES_r for the other complexes. However, as we will see below, the ps and fs time resolved spectroscopic studies cast some doubt upon a model requiring thermally activated ligand dissociation from the reactive excited state.

3.2. Ultrafast (ps and fs) photolysis studies of transient species

With regard to other species along the photochemical reaction coordinate, ultrafast (ps or fs) time resolved spectroscopy has proved necessary to interrogate the structure and dynamics of the excited states and putative geminate and encounter pairs. Such studies often have overlapped with investigations of other diatomic molecules which bind metalloporphyrins, particularly O_2 and CO, the dioxygen complexes being especially of interest owing to the roles of heme proteins in O_2 transfer and storage [76–83]. The present discussion is focused on the nitrosyl complexes, but it is noteworthy that important analogies can be drawn in certain cases between the behaviors of O_2 and NO complexes of metalloproteins.

An early ps photolysis study of nitrosyl hemoglobin by Cornelius et al. [76] found that NO is photodissociated within the laser pulse ($\sim$ 8 ps) to give Hb which largely decayed back to Hb(NO) by 'geminate recombination' processes analyzed in terms of two exponentials, the major component with $\tau \sim 17$ ps the other with $\tau \sim 100$ ps. From similar experiments with the dioxygen and carbonyl Hb complexes, it was discerned that the rates for geminate recombination increased through the series $Hb(CO) > Hb(O_2) > Hb(NO)$ ([71]a). Subsequent studies by Jongeward et al. [77] on nitrosyl complexes of sperm whale and elephant myoglobin Mb(NO) confirm the formation of a short lived transient, consistent with a geminate pair described by the model shown in Fig. 2, and a longer lived but somewhat indefinite separated pair in which the NO wanders through the protein pocket. Again the dioxygen complexes are somewhat similar in behavior, but there was no evidence for fast rebinding of CO upon photolabilization of the carbonyl complexes. Early fs pulse laser experiments by Petrich et al. [78,79] on Hb and Mb complexes of NO and other diatomic molecules conclude that ligand dissociation occurs within 50 fs and that the quantum yields for this process is approximately unity regardless of whether the ligand is NO, O_2 or CO. Fast recombination from a geminate pair was reported as before, but these workers argue that non-exponential decays on the 100 ps time scale, e.g. for myoglobin, occur on the same time scale that photodissociated myoglobin relaxes to the equilibrium deoxy Mb structure. On the other hand, while the above studies and related subsequent investigations [80–82] disagree on certain details, they are consistent with the formation of a {M(P),NO} geminate pair capable of rebinding to return to the original nitrosyl complex as indicated in Fig. 2. From these results, there appears to be a consensus that the small Φ_{dis} (10^{-3}) obtained with ns laser photolysis of nitrosyl hemoproteins originates from the protein structure surrounding heme. NO photodissociated is mostly trapped in a protein pocket and recombines to the nitrosyl hemoproteins at a rate faster than diffusion to fully separated species.

The studies by Petrich et al. [78,79], noted the formation of two heme transients. Transient A has a lifetime of 300 fs; that of transient B is 2.5 ps. The yield ratio, Φ_A Φ_B, of the two was found to differ depending on the nature of the dissociated diatomic ligand. The two transients were ascribed to the d–d^* excited states of the dissociated hemoproteins. The 300 fs component is assumed to be an excited state with a spin state $S = 1$, in which the porphyrin plane is slightly domed. On the other hand, the 2.5 ps component is suggested to be an excited state with a planer porphyrin structure, and it is this species which undergoes fast recombination with O_2 and NO. Along similar lines, the technique of fs coherence spectroscopy on Mb(NO) has been reported to select out and identify low frequency 'reactive' modes attributed to heme doming and iron histidine motion associated with the prompt (< 75 fs) dissociation of the Fe–NO bond and the concomitant spin change of the heme iron and depopulation of its d_{z^2} orbital.

Two ultrafast time-resolved studies of simpler metalloporphyrin systems are noteworthy in the context of the above discussion. Traylor and coworkers [84] used μs and ps flash photolysis to investigate the photolability of a series of model nitrosyl $Fe^{II}(P)$ complexes with imidazole as sixth ligand in toluene, aqueous

1-methylimidazole (1-MeIm), Nujol and glycerol as solvents at 20°C. Quantum yields measured for Eq. (1) demonstrated that Φ_{dis} is relatively insensitive to the nature of the various synthetic porphyrins, some quite sterically crowded, all of which gave values in the range 0.21 to 0.49 in toluene solution. However, varying the solvent, especially solvent viscosity, had a measurable effect on Φ_{dis}, which dropped by an order of magnitude from aqueous 1-MeIm (0.077) to 70% glycerol H$_2$O (0.007) solution for Fe(protoheme)(1-MeIm)(NO). A similar viscosity related effect was seen in comparing quantum yields measured for analogous Fe(P)(NO) complexes in toluene and in Nujol. These experiments were interpreted in terms of geminate pair formation. Substantial increases in viscosity by addition of the highly viscous cosolvent glycerol would lead to decreases in cage escape, hence decreased Φ_{dis} values. Short lived transients consistent with cage recombination ($k_{cg} \sim 9 \times 10^{10}$ s^{-1}) were directly observed by ps spectroscopy in the case of aqueous 1-MeIm (30°) solution suggesting that the M–NO photolabilization yield was ~ 1.0 but only about 10% escapes to the fully dissociated pair under these conditions.

Ultrafast techniques were also used by Morlino and Rodgers to examine the deligation yields and kinetics of Fe(TPP)(NO) and of Co(TPP)(NO) in ambient temperature benzene solutions [85]. For both compounds, dissociation to the separated species M(P) plus NO was found to occur within a few ps. For Fe(TPP)(NO), the dynamic absorption changes monitored at 450 nm during the first 50 ps indicated three exponential decay processes, first a rise in absorbance ($k = 7 \times 10^{11}$ s^{-1}) followed by a biexponential decay (5×10^{11} and 1×10^{11} s^{-1}). Energy transfer experiments using different sensitizers was used to map the relevant excited state energies and the relaxation dynamics during this time frame were interpreted in terms of photophysical processes (Fig. 3). The internal conversion from the initially formed ES ^{2}Q$(\pi\pi^*)$ to the lower energy ^{2}T$(\pi\pi^*)$ was concluded to occur within the 200 fs pulse. So the first observable process, the absorbance rise was argued to represent the partitioning between the unreactive ^{4}T$(\pi\pi^*)$ state (which decays to GS) and the reactive charge transfer state to which is attributed NO labilization.

According to this model, the CT excited state dissociates NO as rapidly as it is formed leaving relaxation of the ^{4}T$(\pi\pi^*)$ to GS and cooling of the vibronically excited Fe(TPP)* to explain the slower exponential decays. The 2-fold higher Φ_{dis} value for Co(TPP)(NO) relative to Fe(TPP)(NO) in fluid solution [71] was attributed to the more efficient decay pathway via ^{4}T$(\pi\pi^*)$ in the latter case. However, recombination of a {M(TPP),NO} geminate pair was not discussed, as it appears that the unadorned photophysical model displayed in Fig. 3 does not address either the temperature effects nor the solvent effects on Φ_{dis} described above for these and related model systems.

Thus, despite some very sophisticated studies of NO photolabilization from nitrosyl metalloporphyrins and related metalloproteins, uncomfortable ambiguities remain. For example, there appears to be general agreement that for the nitrosyl heme proteins, an encounter complex, presumably the caged pair, is first formed from the reactive excited state. The protein inhibits this from diffusing apart thereby reducing quantum yields substantially. However, as noted by Hoffman and
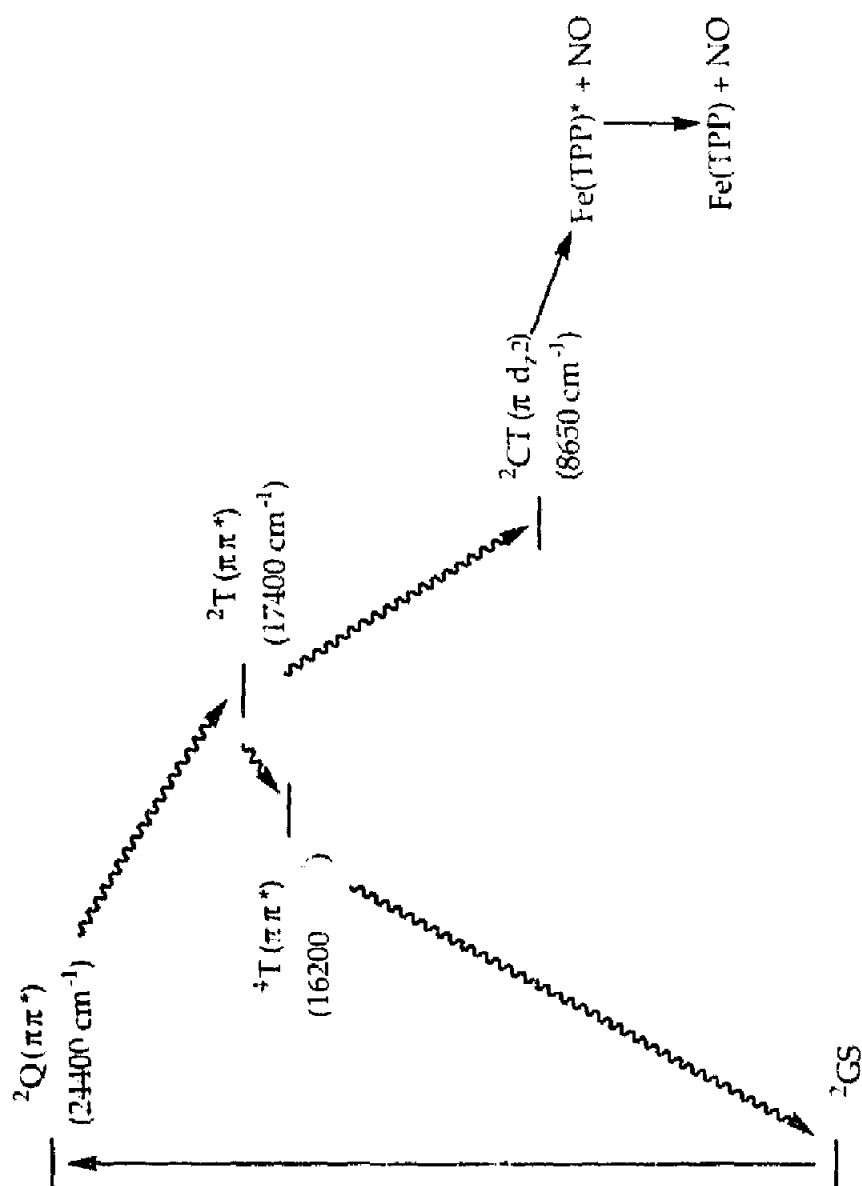
$^2Q(\pi\pi^*)$
(24400 cm^{-1})

$^2T(\pi\pi^*)$
(17400 cm^{-1})

$^4T(\pi\pi^*)$
(16200)

$^2CT(\pi\ d_{z^2})$
(8650 cm^{-1})

Fe(TPP)* + NO

Fe(TPP) + NO

^2GS

Fig. 3. Proposed excited state scheme to explain quantum yields less than unity in the photodissociation of NO from Fe(TPP)(NO) (from Ref. [85]).

Gibson [68], it appears that even in the protein systems, those complexes with $r = 6$ (e.g. $Fe^{II}(CO)$, $Fe^{III}(NO)$, $Mn^{II}(NO)$) often display high net photolabilities relative to analogous $r = 7$ or 8 cases. Perhaps the reason for this lies in the vibronic character of the initially formed caged pair. Does this have a particular distortion trajectory when $r = 6$ which discourages recombination? With regard to the model $M(P)(NO)$ systems a simple question needs to be resolved: do the absorption changes noted in the first 50 ps reflect vibronic cooling of $M(P)$ fragments initially formed, competitive recombination diffusion apart of the caged {M(P),NO} pair or both? Since the fast spectroscopy experiments seem agreed that M–NO bond dissociation occurs on the sub ps time scale, temperature and viscosity effects on ES_1 reactions would seem a less likely explanation than similar influences upon the competitive reactions of the caged pair. The ambiguity partially results from the nature of the experimental observations, which have focused on the strongly absorbing metalloporphyrin chromophore. New insight into the nature of the relevant excited states and intermediates along the reaction coordinate would ensue from sampling the evolution of the NO chromophore, presumably by ultrafast time resolved vibrational spectroscopy.

4. Equilibria and dynamics of the formation of nitrosyl metalloporphyrin complexes

Simple nitrosylation of a metalloporphyrin is expressed by

$$M(P) + NO \rightarrow M(P)(NO) \tag{6}$$

Notably, the activation of soluble guanylyl cyclase involves just such a reaction where the acceptor site of the enzyme is a $Fe^{II}(PPIX)$. Similarly roles such as cytochrome oxidase or catalase inhibition must involve NO reactions with ferro- or ferriheme targets, so a clear understanding of the dynamics and mechanisms of such pathways is essential to understanding the biochemical mechanisms. The kinetics of the nitrosylation of various heme proteins as well as a number of model compounds have been reported as the result of the studies concerned with NO photodissociation mechanisms long before the biological roles of NO were recognized. As discussed in the previous section, one aspect of the interest in nitrosylation was the potential relation of the reaction to the oxygenation of the same proteins. An important question that one might ask here is whether NO, a stable free radical, forms bonds to redox active metals by mechanisms different from the reactions of the same metal complex with various Lewis base ligands? While it is often assumed that reaction of a ligand with heme iron requires an open coordination site, the quantitative basis for such assumption, especially for reaction with NO, is more legendary than factual. This point is not strictly hypothetical given the report by Armor et al. [86] that NO reacts with the hexacoordinate d^5 complex $Ru(NH_3)_6^{3+}$ to give $Ru(NH_3)_5(NO)^{3+}$ with a second order rate ($k = 0.19$ M^{-1} s^{-1}) significantly exceeding the liability of the coordinated ammines. This has been interpreted in terms of an associative mechanism where NO reacts by forming a bond to the ruthenium prior to loss of the NH_3 eventually displaced.

Since photodissociations of NO from nitrosyl metalloporphyrins are usually reversible, ns pulsed laser techniques are well suited for investigating the kinetics of the nitrosylation reaction. In such studies, flash photolysis is used to labilize NO from the M(P)(NO) precursor, and relaxation of the non-steady state system back to equilibrium (Eq. (7)) is monitored spectroscopically.

$$M(P) + NO \underset{k_{off}}{\overset{k_{on}}{\rightleftharpoons}} M(P)(NO) \tag{7}$$

Under excess NO the transient spectra would decay exponentially (k_{obs}) if no permanent photoproduct is formed and the following relationship should hold true.

$$k_{obs} = k_{on}[NO] + k_{off} \tag{8}$$

such that a plot of k_{obs} vs. [NO] would be linear with a slope k_{on} and an intercept k_{off} as illustrated in Fig. 4 [87]. This figure represents kinetics determined thus for a ferriheme compound for which spontaneous ligand dissociation reaction has an appreciable rate constant (k_{off}). In such cases, the ratio of the rate constants k_{on}/k_{off} equals the equilibrium constant K for the formation of the nitrosyl complex under these conditions. However, for many of the systems, especially those of ferroheme complexes or proteins, the 'off' reaction is exceedingly slow, and k_{on} can be determined from the second order relaxation kinetics without added NO.

In such manner the post-photolabilization relaxation rates have been reported for a number of nitrosyl metalloporphyrins and metalloproteins under ambient conditions. For example, in 1979 Tamura et al. [88] reported the k_{on} for reaction of NO with ferri-horseradish peroxidase to have a value of 2×10^5 M^{-1} s^{-1} at pH 8 which could be reproduced by stopped flow kinetics methods. Examples of such rates measured are summarized in Table 2 [69,73,89,90].

4.1. Nitrosylation of M(TPP) (M = Fe^{II} Co^{II}, and Mn^{II}) in toluene solutions

These rates were measured by laser flash photolysis of M(TPP)(NO) in the absence of excess NO [71]. Since the decay of M(TPP) follows second order kinetics, the bimolecular rate constants k_{on} (e.g. Table 2) were directly obtained from the decay analysis of the transient M(TPP). By measuring k_{on} at various temperatures, the activation parameters for the reaction of NO with M(TPP) were obtained (Table 3) [71,90,91]. Table 3 also reports similar data for the OEP complexes of Co^{II} and Mn^{II}.

The activation energies for the TPP complexes are in the order Mn(TPP)(NO) > Fe(TPP)(NO) > Co(TPP)(NO). The nitrosylation changes the spin state ($S = \Sigma m_s$) of the central metal in metalloporphyrin. The spin states of the Mn^{II}TPP, Fe^{II}TPP and Co^{II}TPP complexes are $S = 5/2$, 2 and 1/2, respectively, while those of the nitrosylated M(TPP)(NO) products are 0, 1/2 and 0. From this viewpoint, the manganese complex, which displays the smallest k_{on} value, undergoes the greatest reorganization of spin multiplicity. The slower rates (Table 3) are reflected by both the larger $\Delta H^{\ddagger}$ and more negative $\Delta S^{\ddagger}$ values.

4.2. Nitrosylation and denitrosylation kinetics of ferri- and ferro-hemoproteins

As noted earlier, iron(III) porphyrins react reversibly with NO. The equilibrium constants have been determined for $Fe^{III}(TPPS)$, Mb^{III}, Cyt^{III}, and Cat^{III} by the kinetic flash photolysis technique ($K = k_{on}/k_{off}$) and by spectroscopic titration in aqueous media and are in reasonable agreement (Table 2). The K value for $Fe^{III}(TPPS)$ is one to two orders of magnitude smaller than for the ferrihemoproteins studied. Table 2 also summarizes the dramatic range of k_{on} and k_{off} values obtained by laser flash photolysis of the nitrosyl adducts of $Fe^{III}(TPPS)$ and ferrihemoproteins as well as those of $Fe^{II}(TPPS)$ and some related ferrohemes [73]. For the ferrous complexes, k_{off} values were too small to determine by the flash photolysis method and have to be measured by other means. The small values of k_{off} lead to very larger association constants K for the ferrous species with the exception of Cyt^{II}, which also displays a very small k_{on} value. For example, NO binds deoxyhemoglobin with a K some three orders of magnitude larger than that for CO.

For the ferriheme compounds, the forward rate constants k_{on} are in the order $Cat^{III} > Fe^{III}(TPPS) > Mb^{III} \gg Cyt^{III}$ [73]. A logical argument for the much lower
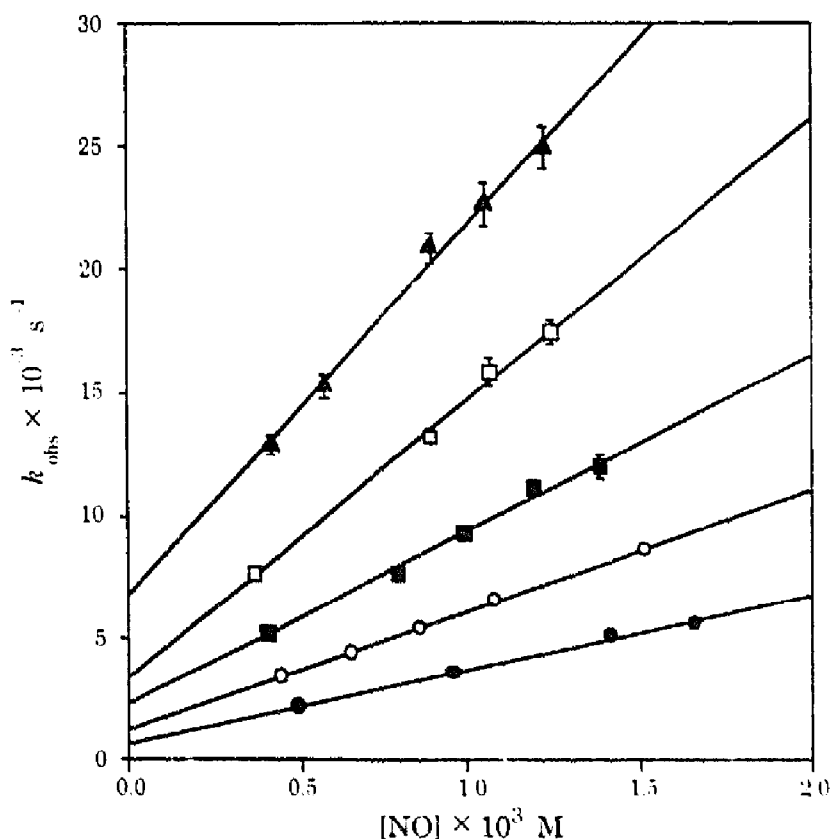
Fig. 4. Plot of k_{obs} vs. [NO] at different temperatures for relaxation of the $Fe^{III}(TMPS)(H_2O)NO)^{2-}$ system after 355 nm flash photolysis. The slopes are k_{on}; the intercepts are k_{off}. ● 298 K; 303 K; ■ 308 K; 313 K; ▲ 318 K. TMPS = tetrasulfonatomesitylporphine (from Ref. [87]).

Table 2
Rate constants k_{on} and k_{off} for the nitrosylations of representative metalloporphyrins and metalloproteins

M(P)	Conditions[a]	k_{on} (M⁻¹ s⁻¹)	k_{off} (s⁻¹)	k_{on}/k_{off} (K)[b] M⁻¹	Ref.
Fe^{III}(TPPS)	H$_2$O, pH 6.5	7.2×10^5	6.8×10^2	1.1×10^3 (1.1×10^3)	[73]
Mb^{III}	H$_2$O, pH 6.5	1.9×10^5	13.6	1.4×10^4 (1.4×10^4)	[73]
Cyt^{III}	H$_2$O, pH 6.5	7.2×10^2	4.4×10^{-2}	1.6×10^4 (1.6×10^4)	[73]
Cat^{III}	H$_2$O, pH 6.5	3.0×10^7	1.7×10^2	1.8×10^5 (1.8×10^5)	[73]
Fe^{II}(TPPS)	H$_2$O, pH 6.5	1.8×10^9	~ 0	$> 10^9$	[73]
Hb^{II}	Phosphate buffer, pH 7.0, 20°C	2.5×10^7	4.6×10^{-3}	5.3×10^{11}	[89]
Mb^{II}	Phosphate buffer, pH 7.0, 20°C	1.7×10^7	1.2×10^{-4}	1.4×10^{11}	[89]
Cyt^{II}	H$_2$O	8.3	2.9×10^{-7}	2.9×10^7 (2.9×10^7)	[73]
Mn^{II}(TPP)	Ethanol	4.9×10^5			[90]
Mn^{II}(TPP)	Toluene	5.3×10^5			[90]
Fe^{II}(PP)(1-MeIm)	Tris buffer, pH 9.0	1.8×10^8	2.9×10^{-4}	6.2×10^{11} (5.8×10^{11})	[69]

[a] All at ambient temperature unless otherwise noted.

[b] The numbers in parenthesis are the equilibrium constants determined directly from spectrophotometric titrations.

reactivity of both Cyt^{III} and Cyt^{II} toward NO, as indicated by the smaller k_{on} values is the occupation of the axial sites on the ferric ion center by an imidazole nitrogen and a methionine sulfur of the protein. However, in contrast to Cyt^{III} and Mb^{III}, Cat^{III} is more reactive than Fe^{III}(TPPS), indicating that in this case, the protein accelerates the nitrosylation. The backward rate constants k_{off} of Mb^{III},

Table 3
The rate constants k_{on} (298 K) and activation parameters for reactions of M(P) (P = TPP or OEP) with NO in toluene solution determined from second order relaxation of flash photolysis transients[a]

	Fe^{II}(TPP)	Co^{II}(TPP)	Mn^{II}(TPP)	Co^{II}(OEP)	Mn^{II}(OEP)
k_{on} (M⁻¹ s⁻¹)	5.2×10^8	2.5×10^9	3.3×10^5	2.3×10^8	3.0×10^5
$\Delta H^\ddagger$ (kJ mol⁻¹)[b]	2.6	1.2	9.3	3.4	5.9
$\Delta S^\ddagger$ (J mol⁻¹ K⁻¹)[b]	−51	−61	−72	−55	−82

[a] From Ref. [71].

[b] Calculated from the Arrhenius activation energies according to Ref. [91].

[c] A higher value of k_{on} (5×10^5 M⁻¹ s⁻¹) was recently measured (Ref. [90]) using competitive trapping to intercept a Mn^{II}(TPP) intermediate generated by photoreduction of Mn(TPP)ONO in toluene. The origins of these differences remain to be resolved.

Cyt[III], and Cat[III] are all smaller than that of Fe[III](TPPS) suggesting retardation of NO dissociation by the proteins.

The small value of k_{off} for the ferroheme proteins is of biological interest with regard to the question of how a ferroheme enzyme such as soluble guanylyl cyclase, once activated by forming an NO complex, undergoes denitrosylative down regulation. Kharitonov et al. [92] have used stopped flow kinetics techniques to determine the first order loss of NO from sGC-NO and measured a rate constant of $\sim 7 \times 10^{-4}$ s^{-1} in pH 7.4 buffered solution at 20°C. This rate is comparable to those noted for various ferroheme proteins listed in Table 2, but is much slower than appropriate for the down regulation mechanism. However, in the presence of both the enzyme substrate guanylyl triphosphate (GTP, 5 mM) and Mg^{2+} (3 mM) the rate was about 70-fold faster ($k \sim 5 \times 10^{-2}$ s^{-1}), although with GTP alone the rate acceleration was only $\sim$ 10-fold. In a similar context, Bohle and coworkers [93] [94], have demonstrated that varying the electronic and stereochemical properties of porphyrin substituents can strongly influence the rates of the displacement of NO from Fe(P)(NO) by nitrogen bases in toluene solution (Eq. (9)). For example, the k_{obs} value for Fe(TPP)(NO) in the presence of 12.4 M pyridine (4×10^{-5} s^{-1}) is nearly six orders of magnitude slower than that measured in 0.1 M pyridine for the Fe(P)(NO complex where P = octabromotetraphenylporphyrin (OBTPP). The kinetics of the Fe(OBTPP) reactions show saturation behavior in [L] and the mechanism is suggested to involve reversible equilibrium formation of Fe(OBTPP)(L)(NO) followed by rate limiting NO dissociation from this species. Such considerations demonstrate the biological relevance of delineating not only the dynamics but also the mechanisms of the nitrosylations and the denitrosylations of the metalloporphyrin models and key metalloproteins.
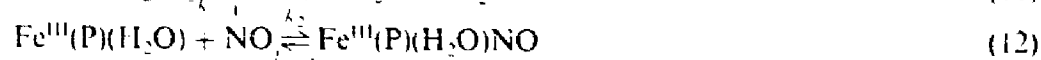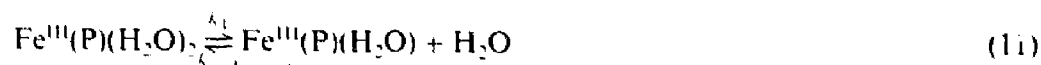
$$\text{Fe(P)(NO)} + 2L \rightarrow \text{Fe(P)L}_2 + NO \tag{9}$$

4.3. Activation parameters for the reactions of NO with ferrihemes

As noted above, despite numerous kinetics measurements of NO reactions with various hemes, the thermal mechanisms by which NO forms and breaks bonds to the metal centers are not well characterized. To probe such pathways, the earlier flash photolysis investigations of Eq. (10) (P = TPPS or TMPS)

$$\text{Fe}^{III}(P) + NO \underset{k_{off}}{\overset{k_{on}}{\rightleftharpoons}} \text{Fe}^{III}(P)(NO) \tag{10}$$

in aqueous solution were extended to a detailed mechanism examination of the on and off reactions [95]. This involved systematic measurements of k_{on} and k_{off} as functions of the temperature (25–45°C) (Fig. 4) and hydrostatic pressure (0.1–250 MPa) (Fig 5) to determine $\Delta H^{\ddagger}$, $\Delta S^{\ddagger}$ and $\Delta V^{\ddagger}$ for both (Table 4) [95–98].

The large and positive $\Delta S^{\ddagger}$ and, more emphatically, $\Delta V^{\ddagger}$ values for k_{on} and k_{off} represent signatures for a substitution mechanism dominated by ligand dissociation, i.e.

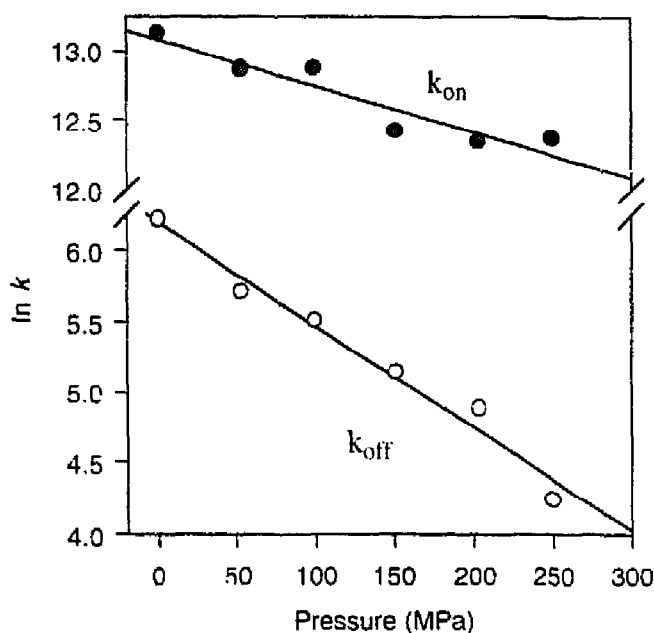$$\text{Fe}^{III}(P)(H_2O)_2 \underset{k_{-1}}{\overset{k_1}{\rightleftharpoons}} \text{Fe}^{III}(P)(H_2O) + H_2O \tag{11}$$

$$\text{Fe}^{III}(P)(H_2O) + NO \underset{}{\overset{k_2}{\rightleftharpoons}} \text{Fe}^{III}(P)(H_2O)NO \tag{12}$$

Fig. 5. Plots of $\ln k_{on}$ (●) and $\ln k_{off}$ (○) vs. hydrostatic pressure P to determine activation volume values $\Delta V^{\ddagger}_{on}$ and $\Delta V^{\ddagger}_{off}$ (from Ref. [87]).

Consistent with this mechanism is the report by Hunt et al. [99] that H_2O exchange between solvent and $Fe^{III}(TPPS)(H_2O)_2^{3-}$ occurs at a first order rate ($k_{ex} = 1.4 \times 10^7$ s^{-1} in 25°C water) far exceeding the k_{obs} values determined at any [NO]. If the steady state approximation were taken with regard to intermediate $Fe^{III}(P)(H_2O)$, the k_{obs} for the exponential relaxation of the non-equilibrium mixture generated by the flash photolysis experiment would be,

$$k_{obs} = \frac{k_1 k_2 [NO] + k_{-1} k_{-2} [H_2O]}{k_{-1} [H_2O] + k_2 [NO]} \tag{13}$$

Table 4
Activation parameters for reaction of NO with $Fe^{III}(TMPS)$ and $Fe^{III}(TPPS)^a$

$$Fe^{III}(P) + NO \underset{k_{off}}{\overset{k_{on}}{\rightleftharpoons}} Fe^{III}(P)(NO)$$
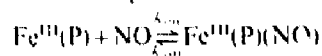
	$Fe^{III}(TPPS)$		$Fe^{III}(TMPS)$		$Mb^{III b}$	
	k_{on}	k_{off}	k_{on}	k_{off}	k_{on}	k_{off}
$\Delta H^{\ddagger}$ (kJ mol^{-1})	62	83	70	78	66	74
$\Delta S^{\ddagger}$ (J mol^{-1} K^{-1})	86	89	100	67	68	34
$\Delta V^{\ddagger}$ (cm^3 mol^{-1})	13	18	8.3	17.9		

a Ref. [95].
b Ref. [96].
$\Delta V^{\ddagger} = -RT(d \ln(k_i)/d P)_T$, where k_i is the rate constant at a particular P [97,98]

Under the experimental conditions, one may conclude that $k_{-1}[H_2O] \gg k_2[NO]$ since both steps involve nearly diffusion limited trapping of an unsaturated metal center and $[H_2O] \gg [NO]$. Accordingly, $k_{on} = k_1 k_2 / k_{-1}[H_2O]$ and $k_{off} = k_{-2}$. In this context, the apparent activation parameters for k_{on} would be sums of terms, e.g.

$$\Delta S^{\ddagger}_{on} = \Delta S^{\ddagger}_1 + \Delta S^{\ddagger}_2 - \Delta S^{\ddagger}_{-1} \text{ and } \Delta V^{\ddagger}_{on} = \Delta V^{\ddagger}_1 + \Delta V^{\ddagger}_2 - \Delta V^{\ddagger}_{-1} \qquad (14)$$

Since the k_2 and the k_{-1} steps represent similar (very fast) reactions of the unsaturated intermediate $Fe^{III}(P)(H_2O)$ with an incoming ligand (NO and H_2O, respectively), the differences in their activation parameters (e.g. $\Delta S^{\ddagger}_2 - \Delta S^{\ddagger}_{-1}$ and $\Delta V^{\ddagger}_2 - \Delta V^{\ddagger}_{-1}$) should be small. In such a case the principal contributor to $\Delta S^{\ddagger}_{on}$ would be $\Delta S^{\ddagger}_1$, the activation entropy for the H_2O dissociative step. The k_1 step should thus display a positive $\Delta H^{\ddagger}_1$ reflecting the energy necessary to break the $Fe^{III}-OH_2$ bond, a large, positive $\Delta S^{\ddagger}_1$ owing to formation of two species from one without a significant change in solvation, and a substantially positive $\Delta V^{\ddagger}_1$ for the same reason. These conditions are met for the k_{on} activation parameters for both complexes (Table 4). Furthermore, the values of $\Delta H^{\ddagger}_{ex}$ (57 kJ mol^{-1}) and $\Delta S^{\ddagger}_{ex}$ (84 J K^{-1} mol^{-1}) for the H_2O exchange [99] on $Fe^{III}(TPPS)(H_2O)_2^{3-}$ are very similar to the respective k_{on} activation parameters. Thus, it was concluded [95] that the reaction parameters in this case are largely defined by a dissociative mechanism. The key point is that for the 'on' reaction with the $Fe^{III}(P)(H_2O)_2^{3-}$ complexes, NO apparently displays reaction kinetics properties quite similar to those for H_2O owing to the dominance of ligand dissociation in determining the behavior of k_{on}.

Although pressure studies have not yet been successful in elucidating the $\Delta V^{\ddagger}$ values for the reaction of NO with a ferriheme protein, the $\Delta H^{\ddagger}$ and $\Delta S^{\ddagger}$ values for Mb^{III} are sufficiently similar to those of the $Fe^{III}(P)$ model compounds in aqueous solution to suggest similar mechanisms (Table 4) [96].
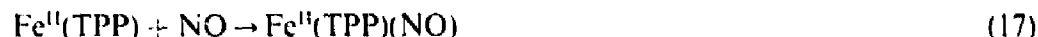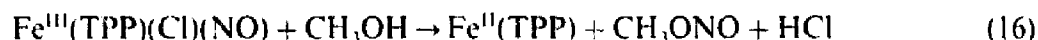
The principle of microscopic reversibility argues that the k_{off} pathway proceeds via the same intermediates. However, having activation parameters similar to those of k_{on} is not a requirement. Since the energetically dominant k_{-2} step involves NO dissociation from a diamagnetic complex which can be formulated as $Fe^{II}(P)(H_2O)(NO^+)$ to the paramagnetic species $Fe^{III}(P)(H_2O)$ plus NO, the reaction coordinate must also incorporate entropic and volume differences accompanying the solvation changes as charge redistributes and the spin cross-over. This may explain why $\Delta V^{\ddagger}_{off}$ is more positive than $\Delta V^{\ddagger}_{on}$ in both cases. However regardless of such speculation, these activation parameters remain consistent with the limiting mechanism described by Eqs. (11) and (12).

On the larger scheme of things, the k_{on} values for Fe(II) and Fe(III) heme proteins range more than eight orders of magnitude (Table 2). Based on these kinetics studies and the activation parameter measurements, it is clear that facile reaction of NO with metal centers requires either a very labile coordination site, as in high spin Fe^{III} heme centers such as $Fe^{III}(TPPS)(H_2O)_2^{3-}$ and catalase $(k_{on} = 3.0 \times 10^7 M^{-1} s^{-1})$, or a vacant coordination site, as in high spin Fe^{II} heme of myoglobin $(1.7 \times 10^7 M^{-1} s^{-1})$ and, presumably, s-GC. This suggests that the free radical nature of NO, which clearly has utmost importance in determining the stability and chemical properties of biologically relevant metal nitrosyl complexes,

has but minor influence on the dynamics of reactions to form such complexes. Since the odd electron resides in a NO π^* orbital, its involvement with the metal center is unlikely to be significant except at short distances where coordination is largely accomplished. In other words, in its on reactions with Fe^{II} and Fe^{III} hemes, NO may act as a normal two electron donor ligand in its initial interaction with the metal center.

5. Reductive nitrosylations of metalloporphyrins

Iron(III) porphyrins and other redox active metal centers have long been known to undergo the reductive nitrosylation in the presence of excess NO [57,100–105]. For example, the synthetic iron(III) porphyrin, $Fe^{III}TPP(Cl)$, in toluene containing a small amount of methanol, undergoes reductive nitrosylation to give $Fe^{II}TPP(NO)$ [57]. It was suggested that the reaction proceeds as shown in Eqs. (15)–(17) [57].

$$Fe^{III}(TPP)Cl + NO \rightleftharpoons Fe^{III}(TPP)(Cl)(NO) \tag{15}$$

$$Fe^{III}(TPP)(Cl)(NO) + CH_3OH \rightarrow Fe^{II}(TPP) + CH_3ONO + HCl \tag{16}$$

$$Fe^{II}(TPP) + NO \rightarrow Fe^{II}(TPP)(NO) \tag{17}$$

In the same context, when an aqueous solution of ferri-hemoglobin, Hb^{III}, is exposed to NO, the product is the NO adduct of ferro-hemoglobin, $Hb^{II}(NO)$ [102]. Reductive nitrosylations of ferrihemoproteins are common, and from a practical perspective, such reactions are important in processes responsible for the curing of meat by NO_2 [106].

In order to gain a better insight into the reaction mechanism, kinetics studies were carried out on the reductive nitrosylation of the ferriheme proteins Cyt^{III}, Mb^{III}, and Hb^{III} in aqueous solutions at various pH [107]. For example, Cyt^{III} undergoes reduction by NO to Cyt^{II} in aqueous solutions at pH values > 6.5. A hypothetical reaction mechanism based on the assumption that NO coordinated to Cyt^{III} is electrophilic toward reaction with OH^- is shown in Scheme 1. Since, as mentioned above, the reaction of NO with Cyt^{II} is very slow, Cyt^{II} can be observed directly and the rates for its formation are functions of [NO] and [OH] as predicted by Eq. (18) [107].

$$\frac{d[Fe^{II}]}{dt} = k_d \frac{K_{NO}[NO]}{1 + K_{NO}[NO]} \frac{K_{OH}[OH^-]}{1 + K_{OH}[OH]} [Fe^{III}(P)] \tag{18}$$

According to Eq. (18), $k_{obs} = k_{OH} \times K_{NO}[NO][OH^-] / (1 + K_{NO}[NO])$ at low pH, where $k_{OH} = k_d \times K_{OH}$, while at high [NO], $k_{obs} = k_{OH}[OH^-]$. Fig. 6 illustrates the response of k_{obs} to [OH] for the NO reduction of Cyt^{III}. No evidence for the N-bound nitrous acid complex was found for any of the ferriheme proteins studied, and at constant [NO] the rate of formation of Cyt^{II} displays a simple first order dependence on [OH]. Thus, either the formation of this intermediate is rate limiting, or K_{OH} is small. Values of K_{NO} were determined from the spectroscopic
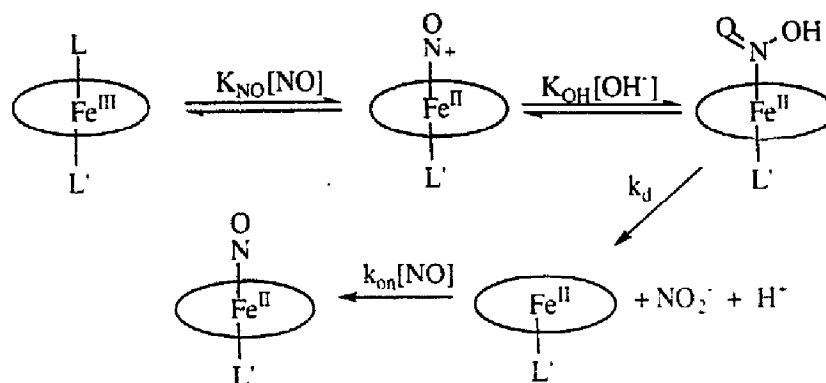
Scheme 1.

titration of Cyt[III] by NO, and the kinetic analysis of the formation of ferroheme species gave the values for k_{on} listed in Table 5.

Mb[III] and Hb[III] also undergo reductive nitrosylation. The mechanisms are regarded to be similar to that for Cyt[III]. However, Mb and Hb readily react with NO, thus the reductive nitrosylation of Mb[III] and Hb[III] produce the ferrous forms Mb(NO) and Hb(NO) as the only observable products.

The values K and k_{on} for Mb[III] and Hb[III] in the presence of NO were determined by kinetic analysis for the formation of Mb(NO) and Hb(NO), and these values are summarized in Table 5. In the Mb[III] case. K_{NO} values proved to be pH dependent, decreasing at the higher pHs studied, suggesting that the change in pH brings forth conformation changes in the protein surrounding heme.

Reductive nitrosylation of Hb[III] also occurs at pH < 6, implying that Hb[III](NO)
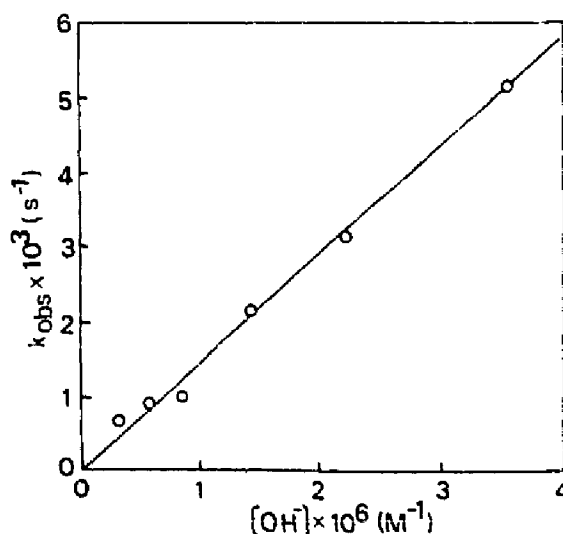

Fig. 6. Rate constants for the formation of Cyt[II] from Cyt[III] in 298 K aqueous solution under a constant pressure of NO (100 Torr) as a function of [OH⁻] (from Ref. [107]).

Table 5
Reductive nitrosylation of ferrihemoproteins[a]

	Cyt[III]	Mb[III]	Hb[III][b]
K_1	1.4×10^4	$(1.3{-}0.62) \times 10^{5c}$	1.3×10^4 M^{-1}
k_{on}	1.5×10^3	3.2×10^2	3.2×10^3 M^{-1} s^{-1}
k_{NO}	8.3	1.7×10^7	2.5×10^7 M^{-1} s^{-1}
pH	6.1–8.45	6.0–7.2	5.6–7.4

[a] Values of constants determined (Ref. [107]).
[b] Hb[III](NO) reacts with H$_2$O in pH 6 water with a rate constant $k_{H_2O} = 1.1 \times 10^{-3}$ s^{-1}.
[c] K_1 for Mb[III] but not for Cyt[III] or Hb[III] is pH dependent dropping to half at higher pH.

reacts with not only OH$^-$ but also with H$_2$O (Eq. (19)). The pseudo first-order rate constant, k_{H_2O} was determined as 1.1×10^{-3} s^{-1} in 25°C water.

$$Hb^{III}(NO) + H_2O \xrightarrow{k_{H_2O}} Hb^{II} + HONO + H^+ \tag{19}$$
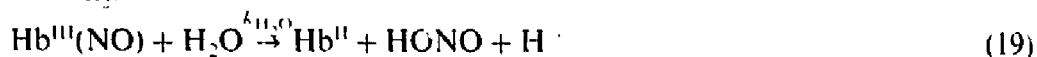
Reductive nitrosylations of Mb[III] and Cyt[III] were not observed at low pH; therefore, direct reactions of Mb[III](NO) and Cyt[III](NO) with H$_2$O are much slower than for Hb[III] [107].

Surprisingly, reductive nitrosylation by NO has been observed for benzene solutions of the Co[III](TPP)(Cl) in the absence of added nucleophiles to give Co[II](TPP)(NO) (M. Hoshino, unpublished results). This reaction was found to occur in benzene, ethanol, ethyl acetate and acetonitrile, irrespective of the nature of solvents used. One might speculate that the reduction is occurring by reductive elimination of ClNO from an initially formed Co[III](TPP)(Cl)(NO), but there is no firm evidence for such a pathway. Analogous reductive nitrosylation was not seen for Mn[III](TPP)(Cl) and Cr[III](TPP)(Cl) in ethanol or benzene (M. Hoshino, unpublished results).

6. Reactions involving dioxygen

The autoxidation of NO in aqueous solution has been subject to several kinetics studies which are generally agreed that the reaction in aqueous solution gives a different stoichiometry than in the gas phase where nitrogen dioxide is the product. In aqueous solution, the nitrogen containing product is nitrite ion, which is probably formed by hydrolysis of intermediates having the stoichiometry N$_2$O$_4$.

$$4NO(aq) + O_2(aq) + 2H_2O \rightarrow 4NO_2^- (aq) + 4H^+ (aq) \tag{20}$$
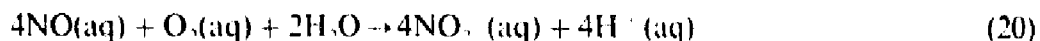
Furthermore, it is generally agreed that the rate law is third order

$$-\frac{d[NO_2^-]}{dt} = 4k_{aq}[NO]^2[O_2] \tag{21}$$

with $4k_{aq} = 9 \times 10^6$ M^{-2} s^{-1} at 25°C [108]. Trapping experiments have detected the presence of intermediates which are both much stronger oxidants and stronger

nitrosating agents than O_2 or NO although various investigators have disagreed on likely identities of these intermediates. The details of these arguments are beyond the scope of this review.

Among those processes potentially able to deplete in vivo NO concentrations are those involving NO, O_2 and some metal species, such as a metalloprotein. For example, it is known that NO reacts rapidly with oxyhemoglobin and with oxymyoglobin to form nitrate plus methemoglobin or metmyoglobin, respectively, [109]

$$Mb(O_2) + NO \rightarrow NO_3^- + Mb^{III} \qquad (22)$$

The second order rate constant for the fast reaction with oxymyoglobin has been reported [110] as 3.7×10^7 M^{-1} s^{-1} and this reaction has been used as a colorimetric test for NO.

In contrast, the reaction of the analogous nitrosyl myoglobin complex with dioxygen,

$$Mb(NO) + O_2 \rightarrow NO_3^- + Mb^{III} \qquad (23)$$

(a reaction of very great importance regarding the stability of cured meats) is much slower [111], although NO complexes with various Fe(II) porphyrins are unstable to autoxidation in aerobic solutions. The kinetics of Eq. (23) were studied by Skibsted et al., who reported that, even at very low dioxygen concentrations, the rate displayed limiting first order behavior with a k_{obs} of 2.3×10^{-4} s^{-1} in 25°C aqueous solution with $\Delta H^{\ddagger} = 110$ kJ mol^{-1} [112]. They proposed that the reaction proceeded via prior formation of an O_2 complex with the nitrosyl myoglobin. However, the proximity of the limiting rate constant to the rate of NO dissociation ($\sim 10^{-4}$ s^{-1}) from Mb(NO) tempts one to think in terms of a mechanism involving this as a first step. Nonetheless, formation of NO_3^- as the nitrogen product indicates that the metal must be involved in the eventual oxidation step, since uncatalyzed NO autoxidation in aqueous media gives nitrite instead. In this context, it is notable that a pressure effect study on the rate of Mb(NO) autoxidation demonstrated a positive $\Delta V^{\ddagger}$ ($+8$ cm^3 mol^{-1}) for this reaction [113].

7. Concluding remarks

The above discussion of the chemistry of metal porphyrin nitrosyl complexes is too brief to do justice to the extensive studies in this area. Furthermore, while the title would appear to be more inclusive, the present article has focused primarily on the very rich mechanistic chemistry of the nitrosyl complexes of the first row transition elements and especially of iron(II) and iron(III) porphyrins, since these systems are of greater interest with regard to possible biological roles of NO. However, although less extensively studied, there is a very rich chemistry of the heavier metal porphyrin nitrosyl complexes as well. For example, a number of ruthenium nitrosyl complexes Ru(P)(L)(NO) have been prepared and characterized [113–119]. Mechanistic studies include investigations of the reactions leading to

formation of these complexes, a particularly interesting reaction being the disproportionation illustrated by [115]:

$$Ru(P)(CO) + 4NO \rightarrow Ru(P)(NO)(ONO) + CO + N_2O \tag{24}$$

Notably, this is quite analogous to observations made in certain reactions of NO with ferric and ferrous porphyrins. The electrochemical [113] and photochemical properties [119,120] of certain of these ruthenium systems have been probed as well; however, the scope of the present review is inadequate to cover these topics.

The interactions of NO with metallo porphyrin centers is clearly relevant to the roles of nitric oxide as a bioregulatory molecule in smooth muscle and nerve tissue and a possibly to its role as a cytotoxin in immune reaction to pathogen invasion. In this context it is notable that despite considerable attention over that past several decades, even simple mechanistic issues such as just how bonds between the metal and the ligand are formed (and broken) and what factors determine the kinetics of these processes are not fully understood. Thus, this subject of inquiry continues to represent a rich mother lode of information ripe for mining and relevant to important biomedical issues.

Acknowledgements

References

[1] B.B. Wayland, J.V. Minkiewicz, M.E. Abd-Elmageed, J. Am. Chem. Soc. 96 (1974) 2795.

[2] I.A. Cohen, B.C. Chow, Inorg. Chem. 13 (1974) 488.

[3] B.B. Wayland, L.W. Olson, Z.U. Siddiqui, J. Am. Chem. Soc. 98 (1976) 94.

[4] J. Cannon, J. Geibel, M. Whipple, T.G. Traylor, J. Am. Chem. Soc. 98 (1976) 3395.

[5] S.K. Cheung, C.J. Grimes, J. Wong, C.A. Reed, J. Am. Chem. Soc. 98 (1976) 5028.

[6] N. Farrell, D.H. Dolphin, B.R. James, J. Am. Chem. Soc. 100 (1978) 324.

[7] B.R. James, in: D. Dolphin (Ed.), The Porphyrins, vol. V, Academic Press, New York, 1979, Part C, Ch. 6.

[8] B.B. Wayland, A.R. Newman, J. Am. Chem. Soc. 101 (1979) 6472.

[9] M. Hoshino, Y. Iimura, S. Konishi, J. Phys. Chem. 96 (1992) 179.

[10] C.K. Chang, T.G. Traylor, Proc. Natl. Acad. Sci. USA 72 (1975) 1160.

[11] J.P. Collman, Acc. Chem Res. 10 (1977) 265.

[12] C.A. Reed, S.K. Cheung, Proc. Natl. Acad. Sci. USA 74 (1977) 1780.

[13] Q.H. Gibson, in: D. Dolphin (Ed.), The Porphyrins, vol. V, Academic Press, New York, 1979, Part C, Ch. 5.

[14] J.P.: Collman, J.I. Brauman, B.L. Iverson, J.L. Sessler, R.M. Morris, Q.H. Gibson, J. Am. Chem. Soc. 105 (1983) 3052.

[15] J.P. Collman, Inorg. Chem. 36 (1997) 5145.

[16] J.-P. Collman, T. Eberspacher, L. Fu, P.C. Herrmann, J. Mol. Catal. A 117 (1997) 9–20.

[17] J.B. Hibbs Jr., Z. Vavrin, R.R. Taintor, J. Immunol. 138 (1987) 550.

[18] L.J. Ignarro, G.M. Buga, K.S. Wood, R.E. Byrns, Proc. Natl. Acad. Sci. USA 84 (1987) 9265.

[19] R.M.J. Palmer, A.G. Ferrige, S. Moncada, Nature 327 (1987) 524.

[20] J.R. Lancaster Jr., J.B. Hibbs Jr., Proc. Natl. Acad. Sci. USA 87 (1990) 1223.

[21] J. Garthwaite, Trends Neurosci. 14 (1991) 60.

[22] L. Ignarro, J. Biochem. Pharmacol. 41 (1991) 485.

[23] F.Y. Liew, F.E.G. Cox, Immunol. Today 17 (1991) A17.

[24] D.S. Bredt, P.M. Hwang, C.E. Glatt, C. Lowenstein, R.R. Reed, S.H. Snyder, Nature 351 (1991) 714.

[25] S. Moncada, R.M.J. Palmer, E.A. Higgs, Pharmacol. Rev. 43 (1991) 109.

[26] P. Klatt, K. Schmidt, G. Uray, B. Mayer, J. Biol. Chem. 268 (1993) 14781.

[27] P.-L. Feldman, O.W. Griffith, D. Stuehr, J. Chem. Eng. News 71 (1993) 26.

[28] D.A. Wink, I. Hanbauer, M.B. Grisham, F. Laval, R.W. Nims, J. Laval, J. Cook, R. Pacelli, J. Liebmann, M. Krishna, P.C. Ford, J.B. Mitchell, Curr. Top. Cell. Regul. 34 (1996) 159.

[29] M. Feelish, J.S. Stamler (Eds.), Methods in Nitric Oxide Research, Wiley, Chichester, UK, 1996.

[30] D.A. Wink, Y. Vodovotz, J. Laval, F. Laval, M.W. Dewhirst, J.B. Mitchell, Carcinogenesis 19 (1998) 711.

[31] T.G. Traylor, V.S. Sharma, Biochemistry 31 (1992) 2847.

[32] R. Radi, Chem. Res. Toxicol. 9 (1996) 828.

[33] S. Kim, G. Deinum, M.T. Gardner, M.A. Marletta, G.T. Babcock, J. Am. Chem. Soc. 118 (1996) 8769 and references therein.

[34] J.N. Burstyn, A.E. Yu, E.A. Dierks, B.K. Hawkins, J.H. Dawson, Biochemistry 34 (1995) 5896.

[35] Y. Minamiyama, S. Takemura, S. Imaoka, Y. Funae, Y. Tanimoto, M. Inoue, J. Pharmacol. Exp. Therapeut. 283 (1997) 1479.

[36] M.W.J. Cleeter, J.M. Cooper, V.M. Darley-Usmar, S. Moncada, A.H.V. Scapira, FEBS Lett 345 (1994) 50–54.

[37] T. Noguchi, J. Honda, T. Nagamune, H. Sasabe, Y. Inoue, I. Endo, FEBS Lett. 358 (1995) 9.

[38] T. Noguchi, M. Hoshino, M. Tsujimura, M. Odaka, Y. Inoue, I. Endo, Biochemistry 35 (1996) 16777.

[39] M. Odaka, K. Fujii, M. Hoshino, T. Noguchi, M. Tsujimura, S. Nagashima, M. Yohda, T. Nagamune, Y. Inoue, I. Endo, J. Am. Chem. Soc. 119 (1997) 3785.

[40] M. Tsujimura, N. Dohmae, M. Odaka, M. Chijimatsu, K. Takio, M. Yohda, M. Hoshino, S. Nagashima, I. Endo, J. Biol. Chem. 272 (1997) 29454.

[41] G.C. Brown, Eur. J. Biochem. 232 (1995) 188.

[42] J.M.C. Ribiero, J.M.H. Hazzard, R.H. Nussenzveig, D.E. Champagne, F.A. Walker, Science 260 (1993) 539.

[43] M.A. Tayeh, M.A. Marletta, J. Biol. Chem. 264 (1989) 19654.

[44] B.R. Crane, A.S. Arvai, R. Gachhui, C.Q. Wu, D. Ghosh, E.D. Getzoff, D.J. Stuehr, J.A. Tainer, Science 278 (1997) 425.

[45] T. Malinski, C. Czuchajowski, in: M. Feelish, J.S. Stamler (Eds.), Methods in Nitric Oxide Research, Wiley, Chichester, UK, 1996, Ch. 22.

[46] D.A. Wink, P.C. Ford, J.S. Beckman, in: M. Feelish, J.S. Stamler (Eds.), Methods in Nitric Oxide Research, Wiley, Chichester, UK, 1996, Ch. 3.

[47] J.H. Enemark, R.D. Feltham, J. Am. Chem. Soc. 96 (1974) 5002.

[48] D.V. Fomitchev, T.R. Furlani, P. Coppens, Inorg. Chem. 37 (1998) 1519.

[49] M.D. Carducci, M.R. Pressprich, P. Coppens, J. Am. Chem. Soc. 119 (1997) 2669.

[50] W.R. Scheidt, J.L. Hoard, J. Am. Chem. Soc. 95 (1973) 8281.

[51] P.L. Piciulo, G. Rupprecht, W.R. Scheidt, J. Am. Chem. Soc. 96 (1974) 5293.

[52] W.R. Scheidt, Y.J. Lee, K. Hatano, J. Am. Chem. Soc. 106 (1984) 3191.

[53] (a) W.R. Scheidt, M.E. Frisse, J. Am. Chem. Soc. 97 (1975) 17. (b) W.R. Scheidt, A.C. Brinegar, E.B. Ferro, J.F. Kerner, J. Am. Chem. Soc. 99 (1977) 7315.

[54] H. Nasri, K.J. Haller, Y. Wang, B.H. Huynh, W.R. Scheidt, Inorg. Chem. 31 (1992) 3459.

[55] J.F. Deatherage, K. Moffat, J. Mol. Biol. 134 (1979) 401.

[56] W.R. Scheidt, L. Piciulo, J. Am. Chem. Soc. 98 (1976) 1913.

[57] X.H. Mu, K.M. Kadish, Inorg. Chem. 27 (1988) 4720.

[58] B.M. Hoffman, C.J. Weschler, F. Basolo, J. Am. Chem. Soc. 98 (1976) 5473.

[59] S. Konishi, M. Hoshino, M. Imamura, J. Phys. Chem. 86 (1982) 1412.

[60] M. Hoshino, S. Konishi, Chem. Phys. Lett. 86 (1982) 228.

[61] B.B. Wayland, L.W. Olson, J. Am. Chem. Soc. 95 (1974) 6037.

[62] H. Kon, Biochem. Biophys. Acta 379 (1975) 103.

[63] T. Yoshimura, Bull. Chem. Soc. Jpn. 64 (1991) 2819.

[64] G. Palmer, in: D. Dolphin (Ed.), The Porphyrins, vol. IV, Academic Press, New York, 1979, Ch. 6.

[65] H. Kon, N. Kataoka, Biochemistry 8 (1969) 4757.

[66] (a) M. Gouterman, J. Mol. Spectrosc. 6 (1961) 138. (b) M. Gouterman, in: D. Dolphin (Ed.), The Porphyrins, vol. III, Academic Press, New York, 1978, Ch. 1.

[67] A. Antonini, M. Brunori, Hemoglobin and Myoglobin in their Reaction with Ligands, North-Holland, Amsterdam, 1971.

[68] B.M. Hoffman, Q.H. Gibson, Proc. Natl. Acad. Sci. USA 75 (1978) 21–25.

[69] E.J. Rose, B.M. Hoffman, J. Am. Chem. Soc. 105 (1983) 2866.

[70] M. Hoshino, S. Arai, M. Yamaji, Y. Hama, J. Phys. Chem. 90 (1986) 2109.

[71] M. Hoshino, M. Kogure, J. Phys. Chem. 93 (1989) 5478.

[72] W.A. Saffran, Q.H. Gibson, J. Biol. Chem. 252 (1977) 7955.

[73] M. Hoshino, K. Ozawa, H. Seki, P.C. Ford, J. Am. Chem. Soc. 115 (1993) 9568.

[74] T. Takano, R.E. Dickerson, J. Mol. Biol. 153 (1981) 95.

[75] F. Sato, Y. Shiro, Y. Sakaguchi, T. Suzuki, T. Iizuka, H. Hayashi, J. Biol. Chem. 265 (1990) 2004.

[76] P.A. Cornelius, R.M. Hochstrasser, A.W. Steel, J. Mol. Biol. 163 (1983) 119.

[77] K.A. Jongeward, D. Magde, D.J. Taube, J.C. Marsters, T.G. Traylor, V.S. Sharma, J. Am. Chem. Soc. 110 (1988) 380.

[78] J.W. Petrich, C. Poyart, J.L. Martin, Biochemistry 27 (1988) 4049.

[79] J.W. Petrich, J.-C. Lambry, K. Kuczera, M. Karplus, C. Poyart, J.L. Martin, Biochemistry 30 (1991) 3975.

[80] M. Ikeda-Saito, Y. Dou, T. Yonetani, J.S. Olson, T. Li, R. Regan, Q.H. Gibson, J. Biol. Chem. 268 (1993) 6855.

[81] M.L. Carlson, R. Regan, R. Elber, H. Li, G.N. Phillips, J.S. Olson, Q.H. Gibson, Biochemistry 33 (1994) 10597.

[82] J.W. Petrich, J.-C. Lambry, S. Balasubramanian, D.G. Lambright, S. Boxer, J.L. Martin, J. Mol. Biol. 238 (1994) 437.

[83] L. Zhu, T. Sage, P.M. Champion, Science 266 (1994) 629.

[84] T.G. Traylor, D. Magde, J.C. Marsters, K.A. Jongeward, G.Z. Wu, K. Walda, J. Am. Chem. Soc. 115 (1993) 4808.

[85] E.A. Morlino, M.A.J. Rodgers, J. Am. Chem. Soc. 118 (1996) 11798.

[86] J.N. Armor, H.A. Scheidegger, H. Taube, J. Am. Chem. Soc. 90 (1968) 5928.

[87] P.C. Ford, J. Bourassa, K. Miranda, B. Lee, I. Lorkovic, S. Boggs, S. Kudo, L. Laverman, Coord. Chem. Rev. 171 (1998) 185.

[88] M. Tamura, K. Kobayashi, K. Hayashi, FEBS Lett. 88 (1978) 124.

[89] E.G. Moore, Q.H. Gibson, J. Biol. Chem. 251 (1976) 2788.

[90] M. Hoshino, Y. Nagashima, H. Seki, M. De Leo, P.C. Ford, Inorg. Chem. 37 (1998) 2464.

[91] A.G. Sykes, Kinetics of Inorganic Reactions, Pergamon, Oxford, 1966, p. 16.

[92] (a) V.G. Kharitonov, M. Russwurm, D. Magde, V.S. Sharma, D. Koesling, Biochem. Biophys. Res. Commun. 239 (1997) 284. (b) V.G. Kharitonov, M. Russwurm, D. Magde, V.S. Sharma, D. Koesling, Biochemistry 36 (1997) 6814.

[93] D.S. Bohle, C.-H. Hung, J. Am. Chem. Soc. 117 (1995) 9584.

[94] D.S. Bohle, P. Debrunner, J.P. Fitzgerald, B. Hansert, C.-H. Hung, A. Thomson, J. Chem. Commun. (1997) 91.

[95] L.E. Laverman, M. Hoshino, P.C. Ford, J. Am. Chem. Soc. 119 (1997) 12663.

[96] L.E. Laverman, P.C. Ford, submitted for publication.

[97] D.R. Crane, P.C. Ford, J. Am. Chem. Soc. 113 (1991) 8510.

[98] T.G. Traylor, J. Luo, J.A. Simon, P.C. Ford, J. Am. Chem. Soc. 114 (1992) 4340.

[99] I.J. Ostrich, L. Gordon, H.W. Dodgen, J.P. Hunt, Inorg. Chem. 19 (1980) 619.

[100] D. Keilin, E.F. Hartree, Nature 139 (1937) 548.

[101] A. Ehrenberg, T.W. Szczepkowski, Acta Chem. Scand. 14 (1960) 1684.

[102] J.C.W. Chien, J. Am. Chem. Soc. 91 (1969) 2166.

[103] T. Yoshimura, S. Suzuki, A. Nakahara, H. Iwasaki, M. Masuko, T. Matsubara, Biochemistry 25 (1986) 2436.

[104] (a) D. Gwost, K.G. Caulton, J. Chem. Soc. Chem. Commun. (1973) 64. (b) D. Gwost, K.G. Caulton, Inorg. Chem. 12 (1973) 2095.

[105] D. Tran, B.W. Shelton, Al.H. White, L.E. Laverman, P.C. Ford, Inorg. Chem. 37 (1998) 2505.

[106] H.J. Anderson, L.H.J. Skibsted, J. Agric. Food Chem. 40 (1992) 7041.

[107] M. Hoshino, M. Maeda, R. Konishi, H. Seki, P.C. Ford, J. Am. Chem. Soc. 118 (1996) 5702.

[108] P.C. Ford, D.A. Wink, D.M. Stanbury, FEBS Lett. 326 (1993) 1.

[109] M. Feelisch, Cardiovasc. Pharmacol. 17 (1991) S25.

[110] M.P. Doyle, J.W. Hoekstra, J. Inorg. Biochem. 14 (1981) 351.

[111] H.J. Andersen, L.H. Skibsted, J. Agric. Food Chem. 40 (1992) 1741.

[112] L. Bruun-Jensen, L.H. Skibsted, Meat Sci. 44 (1996) 145.

[113] K.M. Kadish, V.A. Adamian, E.V. Caemelbecke, Z. Tan, P. Tagliatesta, P. Bianco, T. Boschi, G.-B. Yi, M.A. Khan, G.B. Richter-Addo, Inorg. Chem. 35 (1996) 1343.

[114] D.S. Bohle, P.A. Goodson, B.D. Smith, Polyhedron 15 (1996) 3147.

[115] K.M. Miranda, X. Bu, I. Lorkovic, P.C. Ford, Inorg. Chem. 36 (1997) 4838.

[116] G.B. Yi, M.A. Khan, D.R. Powell, G.B. Richter-Addo, Inorg. Chem. 37 (1998) 208.

[117] (a) G.B. Yi, L. Chen, M.A. Khan, G.B. Richter-Addo, Inorg. Chem. 36 (1997) 3876. (b) G.B. Yi, L. Chen, M.A. Khan, G.B. Richter-Addo, Inorg. Chem. 35 (1996) 3453.

[118] S.J. Hodge, L.-S. Wang, M.A. Khan, V.G. Young, G.B. Richter-Addo, J. Chem. Soc. Chem. Commun. (1996) 2283.

[119] C.D. Tait, D. Holten, M.H. Barley, D. Dolphin, B.R. James, J. Am. Chem. Soc. 107 (1985) 1930.

[120] (a) I.M. Lorkovic, K.M. Miranda, B. Lee, S. Bernhard, J.R. Schoonover, P.C. Ford, J. Am. Chem. Soc. 120 (1998) 11674. (b) B. Lee, Ph.D. Dissertation, UC Santa Barbara, CA, 1997.